Int. J. Multiphase Flow Vol. 19, No. 4, pp. 651–664, 1993
Printed in Great Britain.

0301-9322/93 $6.00 + 0.00

DISPERSION OF PARTICLES IN ANISOTROPIC TURBULENT FLOWS

D. BURRY and G. BERGELES

Fluids Section, Department of Mechanical Engineering, National Technical University of Athens, Athens, Greece

(Received 1 November 1992; in revised form 15 March 1993)

Abstract—A Lagrangian approach is used to simulate particle dispersion in anisotropic turbulent flows. Discrete particles are tracked in three dimensions, influenced by the fluid's turbulent velocity fluctuations. The fluctuations are temporally and directionally correlated through a statistical sampling method reflecting the anisotropy of the flow field. They are calculated at the discrete particle's position through a spatial correlation which takes into consideration the anisotropy of the Reynolds stresses. The method is first tested as to the performance of the temporal and directional correlation features and is then combined with a Eulerian scheme and an algebraic Reynolds stress model for the prediction of the carrier phase. The final form of the model is used to predict a two-phase turbulent round jet and a two-phase inert flow from a quarl burner, with swirl. In parallel to these, the method is compared to a previous particle-tracking method based on an isotropic hypothesis.

Key Words: turbulence, two-phase flows, Lagrangian simulation, anisotropy, turbulent velocity correlations

1. INTRODUCTION

In this paper, a method for the simulation of particle-laden flows is presented analytically and tested taking into consideration the effect of the non-isotropic character of the turbulence, particularly on the discrete phase.

When studying the dispersion of particles in turbulent flows there are two general approaches. The Eulerian approach considers both phases as continuous and solves the transport equations for each. An example of such a method can be found in Picart *et al.* (1986). The Lagrangian approach differs in the way that it deals with the particulate phase. A large number of individual particle trajectories is simulated and from these, statistical mean values are computed (Anagnostopoulos & Bergeles 1992).

The problem with the Lagrangian approach is that, in order to simulate a discrete particle's trajectory, the carrier phase's instantaneous turbulent velocity fluctuations must be known at each point of the trajectory. These fluctuations are, of course, time dependent and the only known quantities, which are the Reynolds stresses derived from a turbulence model, are time averaged. Yuu *et al.* (1978) proposed the use of an isotropic turbulent velocity fluctuation which is sampled randomly from a Gaussian PDF with a standard deviation of $(2/3k)^{0.5}$, where k is the carrier phase's turbulent kinetic energy. The period for which the same fluctuation acts on the particle is determined through two time scales: *the eddy lifetime* and *the eddy transit time*; the smallest of which is taken to be the maximum interaction period.

Gosman & Ioannides (1981) defined the two time scales and introduced a method for the prediction of the dispersion of particles in an isotropic turbulent flow. Variations of this method through different definitions of these scales were also presented by Shuen *et al.* (1983a) and Kalio & Stock (1986). However, these models are still based on an isotropic hypothesis for the turbulence and do not account for the temporal correlation of the fluctuations.

Subsequently, Zhou & Leschziner (1991) and Berlemont *et al.* (1990) have proposed two methods for predicting particle dispersion based on Yuu's original idea but having introduced features that account for the temporal correlation of turbulent fluctuations and for anisotropy and cross-correlations. Predictions of particle dispersion in an anisotropic turbulent pipe flow have also been presented by Milojevic (1990), however the model he used does not take into account the anisotropy of the turbulence when tracking the particles.

Berlemont *et al.* (1990) take temporal correlation into account, using a method that relates each Lagrangian time step to several previous ones, while Zhou & Leschziner (1991) propose relating only every two subsequent time steps—believing that this is sufficient for information to be carried along the trajectory. However, if the time step is to be large enough to permit faster calculations or the particle is dense enough to move significantly away from a fluid particle's trajectory in one time step, then the fluid's turbulent velocity fluctuations cannot be considered constant and a spatial correlation of these must be taken into account. This is not considered by Zhou & Leschziner (1991) but will be examined in this paper.

All the features of this model will be presented accompanied by step-by-step testing of each feature and underlining of the differences from other models. The method will also be used to simulate particle behaviour in a two-phase turbulent round jet. Testing the model in three dimensions, an inert flow from an unconfined quarl burner with swirl will also be predicted. In these final tests, a comparison is made between the results of the present model and a previous method which assumes isotropic turbulence.

2. PRESENTATION OF THE MODEL

In the model, three basic features can be identified. The first accounts for the temporal correlation between fluctuating turbulent velocities of the carrier phase, while the second is an extension of the first to account for directional correlation, which is most evident in anisotropic turbulence. The third feature is the spatial correlation used to calculate the fluid velocity's fluctuations at the position of the discrete particle.

2.1. Temporal Correlation

The basis of the Lagrangian approach is the simulation of a simple fluid particle's trajectory. This would also be the trajectory of a discrete particle if it were light enough to follow the flow perfectly. At each time step, the fluid's instantaneous velocity must be known. This velocity consists of the mean velocity which can be found experimentally or from Eulerian predictions of the carrier phase, and of the turbulent velocity fluctuations. It is these time-dependent fluctuating velocities that must be calculated so that the fluid particle's trajectory can be followed. It is obvious, however, that since they are time dependent, two fluctuating velocities calculated for two subsequent time steps must be correlated.

The temporal correlation proposed by Zhou & Leschziner (1991) is accounted for by the time correlation coefficient $R(\delta t)$, which is defined as

$$R(\delta t) = \frac{\overline{u(t)u(t-\delta t)}}{\overline{u^2(t-\delta t)}}. \qquad [1]$$

A commonly used approximation for $R(\delta t)$ is the following Frenkiel function:

$$R(\delta t) = \exp\left[\frac{-\delta t}{(m^2+1)\tau_L}\right]\cos\left[\frac{m\,\delta t}{(m^2+1)\tau_L}\right]. \qquad [2]$$

In [2], τ_L is the Lagrangian time scale and m is a parameter which determines the number of negative loops in the correlation function and is therefore linked to the type of flow under consideration. For this simple case of homogenous isotropic turbulence $m = 0$ can be used, which gives the correlation function an exponential form without negative values. A pipe flow or a grid-generated turbulence would require a different value for m. Picart *et al.* (1986) also elaborate on the required value of m.

Temporal correlation is introduced to the method when turbulent velocity fluctuations at time level t are expressed as

$$\mathbf{v}_t = \{\beta\}\mathbf{v}_{t-\delta t} + \mathbf{d}_t. \qquad [3]$$

The matrix $\{\beta\}$ expresses all effects from previous time steps and the second term expresses the randomness involved in the last time step δt. In one dimension, [3] can be written as (Zhou & Leschziner 1991):

$$u_t = R(\delta t)u_{t-\delta t} + d_t, \qquad [4]$$

where d_t is sampled from the Gaussian conditional PDF:

$$P(d_t) = \frac{1}{\sqrt{2\pi}[\overline{u_t^2} - R^2(\delta t)\overline{u_{t-\delta t}^2}]^{1/2}} \exp\left\{ - \frac{[u_t - R(\delta t)u_{t-\delta t}]^2}{2[\overline{u_t^2} - R^2(\delta t)\overline{u_{t-\delta t}^2}]} \right\}. \quad [5]$$

A simple test of the performance of time correlation in the method can be carried out by predicting the dispersion of a cloud of massless particles discharged from a point source at x_0 and transported by a uniform steam velocity U_0. Turbulence can be assumed to be both homogenous and isotropic (therefore $m = 0$ in [2]) and, according to Hinze (1975), the mean square displacement $\overline{y^2}$ should result as

$$\overline{y^2}(x) = 2\overline{v^2}\tau_L \frac{(x - x_0)}{U_0}, \quad [6]$$

where $\overline{v^2}$ is the mean square fluctuating velocity.

The attempt to predict [6] using the time-correlated method is made by recording the y locations of a significantly large number of particles (in a statistical sense) at given x locations, the number of particles was considered sufficient when the mean value of the y locations at a certain x location became zero. For the graph in figure 1, 100,000 particles were used and the mean y value was 0.5% of x at $x = 1$ m.

The same test is performed for different values of the computational time step varying from 1/10 to 10 times the values of τ_L. The results prove that even when the time step is very small or large, the temporal correlation, and consequently the dispersion, is correctly accounted for by the method.

2.2. *Temporal and Directional Correlations*

The next step is to include a directional as well as a temporal correlation, something that would enable the model to also perform in anisotropic turbulence. Zhou & Leschziner (1991) express the turbulent velocity fluctuations $\mathbf{v}_t = (u_t, v_t, w_t)^T$ as in [3]. When including directional and temporal correlations the correlation coefficients between $\mathbf{v}_t$ and $\mathbf{v}_{t-\delta t}$ are:

$$R_{xx} = \frac{\overline{u_t u_{t-\delta t}}}{\overline{u_{t-\delta t}^2}}, \quad R_{xy} = \frac{\overline{u_t v_{t-\delta t}}}{\overline{u_{t-\delta t} v_{t-\delta t}}}, \quad R_{xz} = \frac{\overline{u_t w_{t-\delta t}}}{\overline{u_{t-\delta t} w_{t-\delta t}}},$$

$$R_{yx} = \frac{\overline{v_t u_{t-\delta t}}}{\overline{v_{t-\delta t} u_{t-\delta t}}}, \quad R_{yy} = \frac{\overline{v_t v_{t-\delta t}}}{\overline{v_{t-\delta t}^2}}, \quad R_{yz} = \frac{\overline{v_t w_{t-\delta t}}}{\overline{v_{t-\delta t} w_{t-\delta t}}},$$

$$R_{zz} = \frac{\overline{w_t u_{t-\delta t}}}{\overline{w_{t-\delta t} u_{t-\delta t}}}, \quad R_{zy} = \frac{\overline{w_t v_{t-\delta t}}}{\overline{w_{t-\delta t} v_{t-\delta t}}}, \quad R_{zz} = \frac{\overline{w_t w_{t-\delta t}}}{\overline{w_{t-\delta t}^2}}. \quad [7]$$

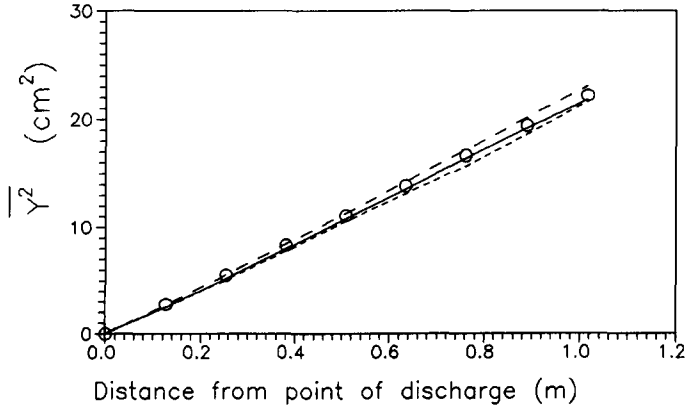

Figure 1. Dispersion of massless particles (Hinze 1975). ○, Hinze's analytical solution; - - - -, $\delta t = 0.1 \cdot \tau_L$, ——, $\delta t = 0.5 \cdot \tau_L$; – – – –, $\delta t = \tau_L$.

Multiplying [3] by $\mathbf{v}^{\mathrm{T}}_{t-\delta t}$ and then time averaging, the matrix $\{\beta\}$ is given by

$$\{\beta\} = \{D\}(\mathrm{covar})^{-1}_{\mathbf{v}_{t-\delta t}}, \tag{8}$$

where $\{D\}$ is related to the Reynolds stresses and correlation functions,

$$\{D\} = \begin{pmatrix} R_{xx}\overline{u^2_{t-\delta t}} & R_{xy}\overline{u_{t-\delta t}v_{t-\delta t}} & R_{xz}\overline{u_{t-\delta t}w_{t-\delta t}} \\ R_{yx}\overline{v_{t-\delta t}u_{t-\delta t}} & R_{yy}\overline{v^2_{t-\delta t}} & R_{yz}\overline{v_{t-\delta t}w_{t-\delta t}} \\ R_{zx}\overline{w_{t-\delta t}u_{t-\delta t}} & R_{zy}\overline{w_{t-\delta t}v_{t-\delta t}} & R_{zz}\overline{w^2_{t-\delta t}} \end{pmatrix}, \tag{9}$$

and $(\mathrm{covar})_{\mathbf{v}_{t-\delta t}}$ is the covariant matrix of $\mathbf{v}_{t-\delta t}$:

$$(\mathrm{covar})_{\mathbf{v}_{t-\delta t}} = \begin{pmatrix} \overline{u^2} & \overline{uv} & \overline{uw} \\ \overline{vu} & \overline{v^2} & \overline{vw} \\ \overline{wu} & \overline{wv} & \overline{w^2} \end{pmatrix}_{t-\delta t}. \tag{10}$$

If the correlation functions are known as in [2] then, as can be seen from the above, it is easy to define $\{\beta\}$. The Lagrangian time scale τ_{L} is given in section 2.3 along with the Eulerian length scale.

It is pointed out that we prefer to non-dimensionalize the correlations with the form used in [7] because, this way when $\delta t \to 0$ and the correlation function of [2] becomes unity, the temporal correlation will become equal to the Reynolds stress at the same instant in time. This does not occur with the form used by Zhou & Leschziner (1991), in which the denominators become $(\sqrt{\overline{u_i^2}}\sqrt{\overline{u_j^2}})$. This leads to rather mistaken calculation of the temporal cross-correlation, especially if this happens to be negative. As will be shown later, this new modification for anisotropic turbulence overcomes the difficulty that arises in the case of negative cross-correlation.

Equation [5] was written only for one dimension but, in fact, it is derived from the three-dimensional PDF:

$$P(\mathbf{d}_t) = \frac{1}{(2\pi)^{3/2}|\mathrm{covar}|^{1/2}_{\mathbf{d}_t}} \exp[-1/2(\mathbf{d}_t)^{\mathrm{T}}(\mathrm{covar})^{-1}_{\mathbf{d}_t}(\mathbf{d}_t)], \tag{11}$$

where $(\mathrm{covar})_{\mathbf{d}_t}$ is the covariant matrix of $\mathbf{d}_t$ and can be calculated in the same way as $(\mathrm{covar})_{\mathbf{v}_{t-\delta t}}$ if [3] is rearranged first:

$$(\mathrm{covar})_{\mathbf{d}_t} = \begin{pmatrix} \overline{d^2_{tx}} & \overline{d_{tx}d_{ty}} & \overline{d_{tx}d_{tz}} \\ \overline{d_{ty}d_{tx}} & \overline{d^2_{ty}} & \overline{d_{ty}d_{tz}} \\ \overline{d_{tz}d_{tx}} & \overline{d_{tz}d_{ty}} & \overline{d^2_{tz}} \end{pmatrix}. \tag{12}$$

Considering $\mathbf{Z}$, a set of random variables with independent standard normal distribution $N(0, 1)$, a sampling method is constructed to perform as the PDF in [11]. This is accomplished when $\mathbf{d}_t$ is written as

$$\mathbf{d}_t = \{b\}\mathbf{Z} \tag{13}$$

and its components are correlated. Because of the symmetry of the PDFs for $\mathbf{Z}$, it is possible to align Z_1 with d_{tx} without affecting the generality of the method. Therefore, it may be considered that $b_{12} = b_{13} = b_{23} = 0$. Multiplying [13] by $\mathbf{d}^{\mathrm{T}}_t$ and then time averaging, the components of $\{b\}$ are found to be:

$$\begin{aligned} b_{11} &= (\overline{d^2_{tx}})^{1/2}, & b_{12} &= 0, & b_{13} &= 0, \\ b_{21} &= \frac{(\overline{d_{tx}d_{ty}})}{b_{11}}, & b_{22} &= (\overline{d^2_{ty}} - b^2_{21})^{1/2}, & b_{33} &= 0, \\ b_{31} &= \frac{(\overline{d_{tx}d_{tz}})}{b_{11}}, & b_{22} &= \frac{(\overline{d_{ty}d_{tz}} - b_{21}b_{31})}{b_{22}}, & b_{33} &= (\overline{d^2_{tz}} - b^2_{31} - b^2_{32})^{1/2}; \end{aligned} \tag{14}$$

so the components of $\mathbf{d}_t$ are easily defined from the random variables Z_1, Z_2, Z_3 and [13], while the values for $\overline{d_{ti}d_{tj}}$ can be found from [3] by multiplying and time averaging. The methodology is presented analytically in Zhou & Leschziner (1991).

If we ignore the temporal correlation for now, ($\{\beta\} = \{0\}$), then [3] leads to $\mathbf{d}_t = \mathbf{v}_t$. Considering the PDF in [11] in two-dimensional space, where $\overline{u^2} = \overline{v^2} = 0.5\ \mathrm{m^2/s^2}$ and $\overline{uv} = 0.0, 0.2, 0.4\ \mathrm{m^2/s^2}$, a very enlightening test can be performed (shown in figure 2). The PDF is plotted (——) for a specific range for the u and v velocities, while the sampling method described above is used to simulate the PDF's behaviour (-----). For each of the three correlation values a total of 200,000 velocity samples were taken, the number of samples to fall inside a predefined area (Δu, Δv) was registered and from them the PDF was reconstructed. The purpose of the test was to determine the effect of different correlation conditions on the sampling method. Zero correlation means that the two velocities are equally liable to take a certain value and, therefore, the value of the velocity vector will be constant. This results in a perfect circle for the PDF in figure 2(a). When correlation exists then a certain value for one velocity predefines the value for the other, depending on the value of the correlation. Thus, when the correlation value becomes larger, the PDF becomes more and more elongated [figures 2(b, c)]. Under all conditions, the sampling method shows good agreement with the plot of the PDF equation [11].

In the next test, both temporal and directional correlation are taken into account. A turbulent field is considered with a constant gradient of the mean velocity $U_0 = A \cdot y (A = \text{const})$. In this field

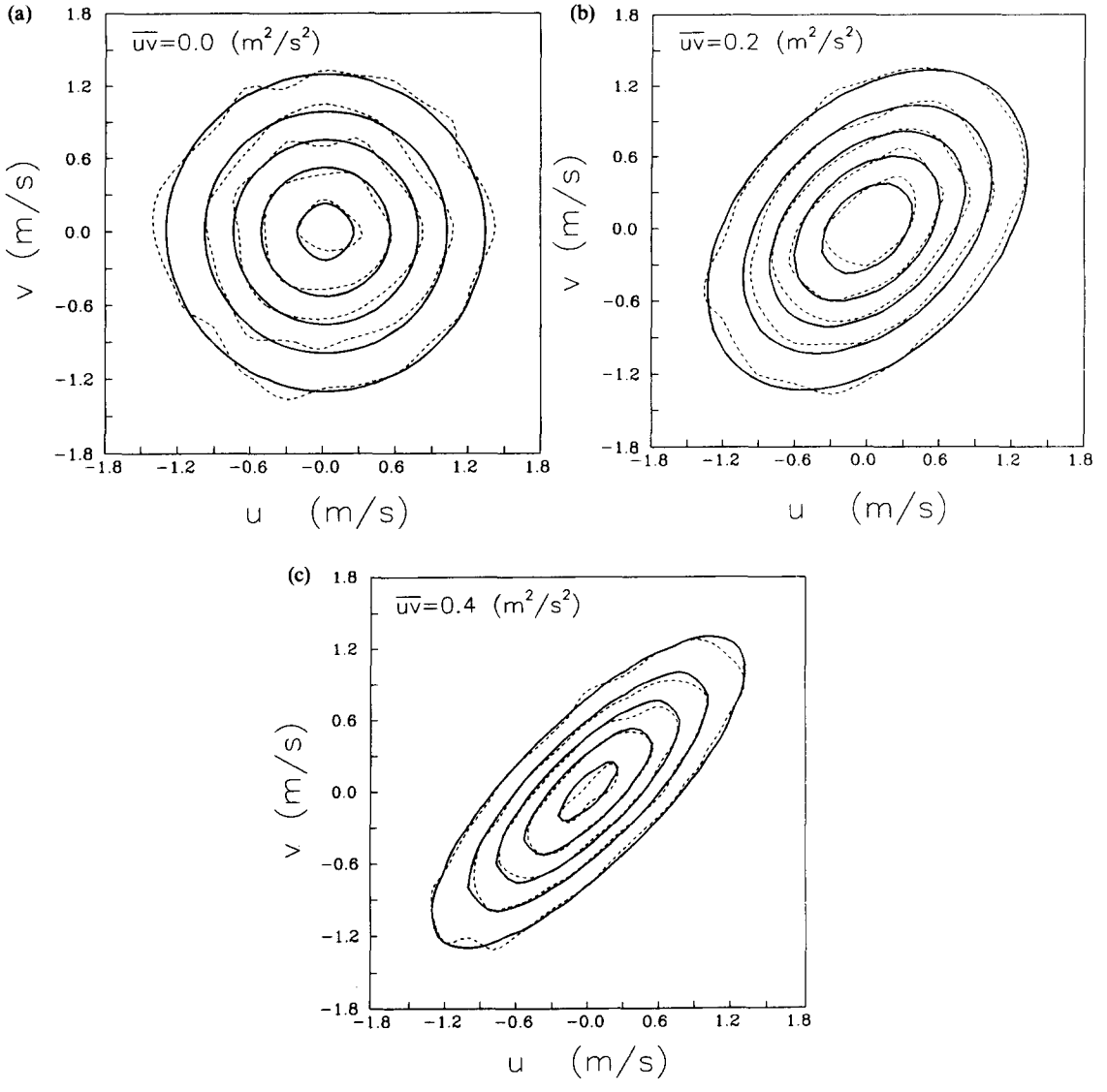

Figure 2(a–c). Reconstruction of conditional PDFs. ——, Plots of the PDF in [11]. ----, Sampling method. PDF values (from innermost curve outwards): (a, b) 0.3, 0.24, 0.18, 0.12, 0.06; (c) 0.05, 0.4, 0.3, 0.2, 0.1.

200,000 fluid particles are released from a point source at $(x, y) = (0, 0)$ under four different conditions. The particles are tracked and their positions are monitored at specific time intervals. The four flow field conditions are:

(i) $U_0 = 0$, $\overline{uv} = 0$. Here there is no mean fluid velocity and no directional correlation of the fluctuating velocities. Particle movement is solely due to turbulent diffusion and, as expected, the contours are concentric circles since no particular direction is favoured [figure 3(a)].

(ii) $U_0 = 0$, $\overline{uv} = -0.4\ \text{m}^2/\text{s}^2$. Of course a situation like this never occurs in nature but it is very explicit as to the influence of the correlation. Again particle movement is due to turbulent diffusion but here it is also influenced by cross-correlation causing the particles to move in a specific direction. The negative value of the cross-correlation performs correctly due to the modification in the correlation functions mentioned previously [figure 3(b)].

(iii) $U_0 = 13 \cdot y$ m/s, $\overline{uv} = 0$. Just like the previous one this situation is not physically realistic. There is no velocity correlation but particle motion is caused by both turbulent diffusion and the flow field's mean velocity. It is interesting to note how the contour is a circle at first but the more the particles move away from the center and are exposed to a greater mean velocity, the contours become more and more elongated [figure 3(c)].

(iv) $U_0 = 13 \cdot y$ m/s, $\overline{uv} = -0.4\ \text{m}^2/\text{s}^2$. This is the most realistic situation of the four. The first contours are influenced more by the correlation since the mean velocity is relatively small in the area close to the source point. As time passes and the particles start to move away, the field's mean velocity plays a more important role, finally becoming more influential than the correlation and gradually changing the direction of the particles' movement [figure 3(d)].

The same tests can be performed in three dimensions, but two dimensions were preferred so that the results could be better evaluated.

2.3. Spatial Correlation

All the tests performed above have been assuming massless Lagrangian fluid particles. According to Zhou & Leschziner (1991), if the time step is sufficiently small then a small and not very dense discrete particle and a fluid particle with the same initial position will not move too far away from each other during that one time step. Therefore, the discrete particle may be followed in one time step, assuming the carrier velocity at the discrete particle's position to be the same as that of the fluid particle. This hypothesis restricts us to small and light particles as well as small time steps. Here, a spatial correlation method will be introduced that will help to overcome such restrictions. Berlemont *et al.* (1990) also include spatial correlation in their approach and the method described below is primarily based on the correlation function that they introduced. However, the principle of the proposed method is quite different.

A discrete spherical particle's trajectory is followed through a modified Riley equation (Berlemont *et al.* 1990) which neglects streamline curvature effects and assumes that the particles are not rotating or interacting. The particles that will be used in the following tests are relatively small and the velocity gradients that appear in the test flows are such as to permit the assumption that Saffman's lift force is negligable. More details on the forces acting on the particle can be found in Smoot & Pratt (1979). The equation is finally given as:

$$\rho_p G_p \frac{dV}{dt} = -\frac{3}{4}\frac{G_p}{d}\rho_f C_D (V-U)|V-U| - \rho_f G_p C_A \frac{d(V-U)}{dt} + G_p(\rho_p - \rho_f)g + \rho_f G_p \frac{DU}{Dt} - \frac{3}{2d} G_p C_H \sqrt{\frac{\rho_f \mu}{\pi}} \int_x^t \frac{\frac{d(V-U)}{dt}}{(t-\tau)^{1/2}} d\tau, \quad [15]$$

where ρ_f and ρ_p are the fluid and particle density, respectively, G_p is the particle volume, U and V are the instantaneous velocity of the fluid and the particle, respectively, d is the particle diameter,

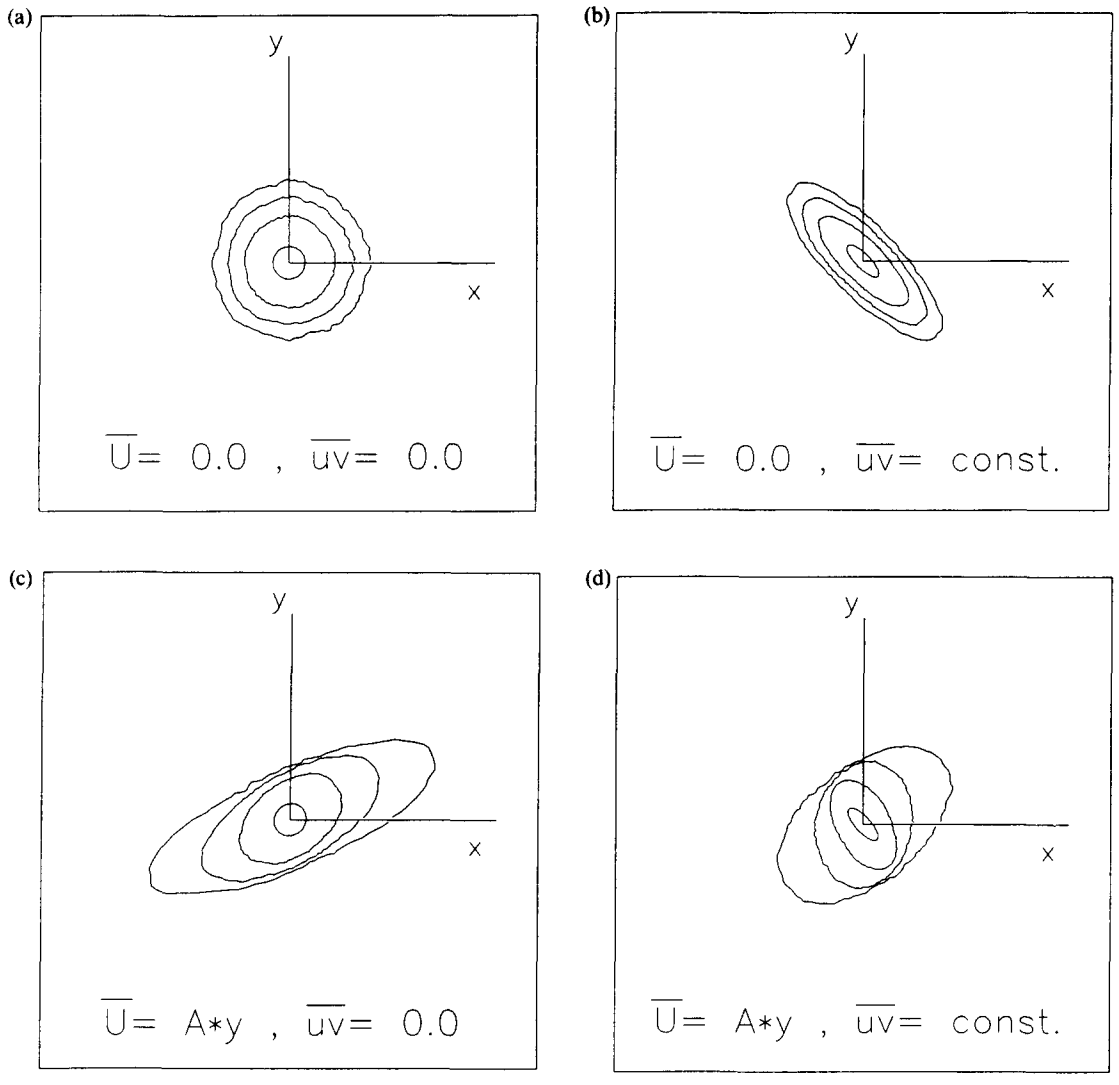

Figure 3(a–d). Tracking of fluid particles in various flow field conditions. Particles released at $t = 0$ s. Lines plotted at $t = 0.02, 0.08, 0.144, 0.216$ s.

g is the acceleration of gravity vector, $\mathrm{d}/\mathrm{d}t$ is along the discrete particle trajectory and $\mathrm{D}/\mathrm{D}t$ is along the fluid trajectory. The C_D, C_A and C_H coefficients are introduced in the original Riley equation to the drag term, the added mass term and the Basset term. As will be discussed later, only the drag term and the gravity term will be used here while the added mass and Basset term are neglected, since we will be dealing with low turbulence intensities and particles whose diameters are smaller than the Kolmogorov scale $(\nu^3/\epsilon)^{1/4}$ and whose densities are much larger than that of the fluid. Mei *et al.* (1991) studied the effect of the Basset term on the behaviour of particles in turbulent fields. They introduced two critical parameters with which to determine how important the Basset term is in a certain flow field. These were taken into consideration before ignoring the Basset term for the present calculations. Finally, the temporal derivatives of the fluid fluctuating velocities can also be neglected because of low turbulence levels.

First, the particle Reynolds number is defined:

$$\mathrm{Re}_p = \frac{|V - U|d}{\nu}; \qquad [16]$$

and for $\mathrm{Re}_p < 200$, C_D becomes

$$C_D = \frac{24}{\mathrm{Re}_p}(1 + 0.15\,\mathrm{Re}_p^{0.687}). \qquad [17]$$

In [15], after the previous assumptions everything is defined so that V at the next time step can be calculated, except for the fluctuating part of U which is the fluid instantaneous velocity at the discrete particle's position. This can be calculated if a spatial correlation is developed between the fluid fluctuating velocities along the trajectory of a fluid particle starting at the same time and position as the discrete particle, and at the discrete particle's position. This could be accomplished using a similar concept to the one used for temporal and directional correlation. So, the fluid fluctuating velocities are connected through

$$\mathbf{v}_p = \{K\}\mathbf{v}_f + \mathbf{e}_t, \tag{18}$$

where the subscripts f and p denote the fluid and the discrete particles' position, respectively. The matrix $\{K\}$ represents the influence of the distance between the two positions and $\mathbf{e}_t$ the randomness involved because of the turbulence. The method remains precisely the same as in section 2.2, except that the correlations R_{ij} are now spatial correlations:

$$R_{ij} = \frac{\overline{u_{ip}u_{jf}}}{u_{if}u_{jf}}, \tag{19}$$

where $i, j = x, y, z$ and denote the three velocity components. The difficulty is in defining the correlations $\overline{u_{ip}u_{jf}}$ between the two positions. Berlemont *et al.* (1990) propose using a Frenkiel family of correlations similar to [2]:

$$\overline{u_{ip}u_{jf}} = \sqrt{\overline{u_{ip}^2}\,\overline{u_{jf}^2}}\exp\left[\frac{-r}{(m^2+1)L_{E_{ij}}}\right]\cos\left[\frac{mr}{(m^2+1)L_{Eij}}\right], \tag{20}$$

where r is the distance between the two positions and L_{Eij} are spatial correlation scales. Here a modification is proposed, expressing the correlations as

$$\overline{u_{ip}u_{jf}} = \overline{u_{if}u_{jf}}\exp\left[\frac{-r}{(m^2+1)L_{E_{ij}}}\right]\cos\left[\frac{mr}{(m^2+1)L_{Eij}}\right]. \tag{21}$$

This modification is felt to be essential, for in the event that a cross-correlation is being calculated ($i \neq j$) [20] cannot deal with the event that the Reynolds shear stress might be negative and therefore, for $r \to 0$, the spatial correlation will not become equal to the real value of the Reynolds shear stress at that point. The expression used in [21] overcomes this problem.

The parameter m is now set to $m = 1$, as is true for the temporal correlations in [2], because the flows to be predicted are more complex and $m = 0$ is no longer a good enough approximation. It should also be noted that in [20] and [21], $i, j = 1, 2, 3$—meaning that the function is true for a different coordinate system where u_1 is collinear to the distance r. This means that certain changes in the coordinate system are required so that spatial correlation can be incorporated. The correlation scales are defined as

$$L_{Eij} = C_{ij}\tau_{Lij}\sqrt{\frac{\overline{u_i^2} + \overline{u_j^2}}{2}}, \quad \tau_{Lij} = C_L\frac{\overline{u_i^2} + \overline{u_j^2}}{2\epsilon}, \tag{22}$$

where C_L is taken to be 0.2 for jets or pipe flows, ϵ is the turbulent energy's rate of dissipation and C_{ij} are constants depending on the scale and the turbulence field. Again, here, there are modifications with relation to both Zhou & Leschziner (1991) and Berlemont *et al.* (1990). The latter use the form u_iu_j instead of $(\overline{u_i^2} + \overline{u_j^2})/2$ which is used in [22]. In the event of negative Reynolds shear stresses this would lead to physically impossible negative values of the Lagrangian cross-time scales. Equations [22] simply consider them to be equal to the mean value of the two relevant normal scales, thus preserving the physical meaning of Lagrangian time scales as the largest interval in time that a Lagrangian particle will continue moving in that particular direction (Hinze 1975).

It should be pointed out that since spatial correlation is dependent on the distance, the correlations become zero if this distance becomes too large. At this point Berlemont *et al.* (1990) use a "correlation domain", meaning that when, and only when, the distance between the positions f and p becomes larger than a length parameter $L_g = C \cdot L_{Eij}$ they start monitoring a new fluid particle from the discrete particle's current position. It is proposed here that a particle may be tracked by ignoring the correlation domain and starting the fluid particle from the discrete particle's position at each time step. This much simpler approach is possible, since even for large and dense

particles the spatial correlation will perform correctly for the distance acquired during one time step. At the same time an unknown parameter (L_g) is dealt with so that the constant C does not have to be arbitrarily defined. However, if there is no experimental data for the Eulerian length scales, a certain degree of uncertainty still holds for the constants in [22]. For the following calculations C_{ij} was taken to be unity.

3. RELIABILITY OF THE COMPLETE DISPERSION MODEL

Having put together the full model it was tested by predicting the experimental results obtained by Shuen *et al.* (1983b) and Hardalupas *et al.* (1990). However, these calculations required a calculation of the flow field taking into consideration the effect of the particles on the flow. This was performed using the basic SIMPLE algorithm with special source terms in the momentum equations to compensate for the momentum and energy exchange from the particles to the carrier phase. Due to this exchange, after the flow field had converged, a statistically large amount of particles (2000–5000) were tracked and then the flow field was recalculated. Usually 3–4 trackings are required, depending on the particle mass loading and the type of flow.

As was mentioned above, the basic advantage of the present model is its ability to account for the anisotropic character of the turbulence. This is achieved through the correlations that have been presented but is also dependent on the Lagrangian time scale and the length scale used in the spatial correlation. The values used for these in the past were given by Gosman & Ioannides (1981) and later by Shuen *et al.* (1983a) as:

$$L_E = C_\mu k^{3/2}/\epsilon, \quad \tau_L = L_E/(2/3k)^{0.5}. \qquad [23]$$

These values were a basic part of the previously used "isotropic" methods which sampled the fluctuations from the same Gaussian PDF as described in the Introduction. A new fluctuation was sampled when the distance between the discrete and fluid particles became larger than the eddy length L_E [23]. This is the "isotropic method", with which results will be compared in the following tests. A complete description of this method (SIMPLE algorithm, particle tracking method etc.) can be found in Anagnostopoulos & Bergeles (1988, 1992), Diakoumakos *et al.* (1988) and Sargianos *et al.* (1990). An intermediate model will also be used for comparison. This will be referred to as "present method A" and includes all the features presented in the previous sections with the difference that the time and length scales will be those in [23] instead of [22], in other words they will be assumed directionally independent. This leads to the same correlation functions for the two (or three) velocity components but does not cripple the model, since the Reynolds stresses will still be calculated separately and thus account for anisotropy. It was first attemped to calculate the Reynolds stresses with Boussinesq's eddy viscosity model. However, serious deviations from physically acceptable results for the stresses led to the use of an algebraic Reynolds stress model. It should be pointed out that correct calculation of these stresses is essential to the model's performance.

3.1. Tests for the Experiments of Shuen et al. (1983b)

Shuen *et al.* (1983b) performed measurements on a free turbulent round jet. The inside diameter of the injector was 10.9 mm and the mean air velocity was 25.22 m/s. The particles that were tracked were 119 μm in diameter and had a density of 2620 kg/m^3, their mean injector exit velocity was 21.89 m/s, while the mass loading was 66%. Results are given in the radial direction for the two measuring positions $X/D = 20$ and 40 and in the axial direction at the centerline. For the prediction of the turbulent flow field, the $(K-\epsilon)$ model was modified according to Launder & Spalding (1974):

$$C_\mu = 0.09 - 0.04f, \quad C_2 = 1.92 - 0.067f, \qquad [24]$$

with

$$f = \left[\frac{Y}{2\,\Delta U}\left(\frac{dU_c}{dx} - \left|\frac{dU_c}{dx}\right|\right)\right]^{0.2},$$

where U_c is the streamwise velocity on the jet axis, Y is the half-width of the jet and ΔU is the radial variation of the velocity over Y.

The present results will be compared to the results obtained by Anagnostopoulos & Bergeles (1988), whose predictions were based on an isotropic hypothesis.

The radial variation of the particles' axial velocity non-dimensionalized by the centerline value is presented in figures 4(a, b) for the axial positions $X/D = 20$ and 40, respectively. As can be seen, there is a significant difference from the isotropic model—especially further away from the symmetry axis. The use of the anisotropic time and length scales (present method B) only slightly improves the predictions. The centerline variation of the particle mass flux non-dimensionalized by the outlet value is presented in figure 5, where the present model performs slightly better in the region near the injector exit and the use of the anisotropic time and length scales leads to an overall better prediction compared to the previous isotropic method. Finally, the particles' turbulent kinetic energy calculated as $k_c = (\overline{u^2} + \overline{v^2} + \overline{w^2})/2$, where $w = v$, is presented in figure 6, where the present method with the anisotropic time and length scales clearly improves the predictions. The initial conditions for the particles were given at $X/D = 1$ (not at the exit position) but there was no data for the particle radial velocities. This was overcome by assuming these velocities equal to those of the carrier phase at that position and could be the cause for the discrepancies near the jet exit. It should be noted that Berlemont *et al.* (1990) overestimate the particle velocities in a similar flow (different mass loading).

3.2. Tests for the Experiments of Hardalupas et al. (1990)

In Hardalupas *et al.* (1990) kerosene droplets, whose density was 780 kg/m^3, were injected into an unconfined quarl burner with a quarl inlet diameter of 16 mm and a quarl exit diameter of 38 mm. The flow had a swirl number of about 0.29 and the cold bulk velocity was 30 m/s. The kerosene flow rate was 0.07 dm^3/min and the size class which will be studied are the 55–60 μm diameter kerosene droplets. The predictions are for inert flow while the X distance is measured from the quarl inlet. This test case was chosen because of the complexity the recirculation zone brings to the flow field. Furthermore, it is a good opportunity to test the model in three dimensions, something that is not presented with previous models neither in Berlemont *et al.* (1990) nor in Zhou & Leschziner (1991).

Particle axial velocities non-dimensionalized by the cold bulk velocity are presented in figures 7(a–c) for the "isotropic model" as presented in Anagnostopoulos & Bergeles (1992), while the use, or not, of anisotropic time and length scales (present methods B and A) surprisingly had a very small effect on the predictions. As can be seen, there is a definite improvement in relation to the isotropic model which underestimated velocities further away from the symmetry axis.

4. COMPUTATIONAL DETAILS

The computational grids used for the tests in section 3 were:

(i) For Shuen *et al.* (1983b), computations were carried out for both 100 × 50 and 40 × 20 grids [Anagnostopoulos & Bergeles (1988) used a 60 × 30 grid] without

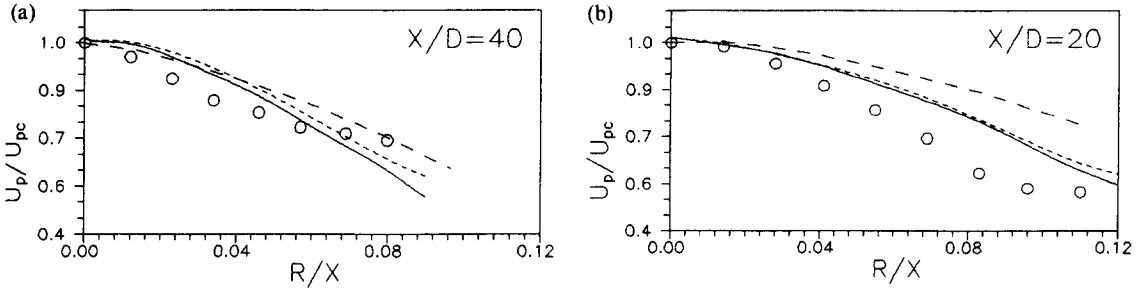

Figure 4(a, b). Particle axial velocities (Shuen *et al.* 1983b). ○, Experiment (Shuen *et al.*); – – –, Anagnostopoulos & Bergeles (1988); - - - -, present method A; ——, present method B.

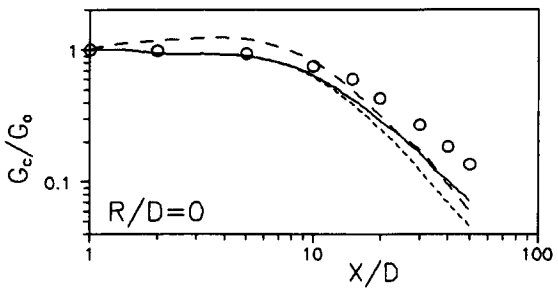

Figure 5. Particle centerline mass flux (Shuen *et al.* 1983b). O, Experiment (Shuen *et al.*); ----, Anagnostopoulos & Bergeles (1988); ----, present method A; ——, present method B.

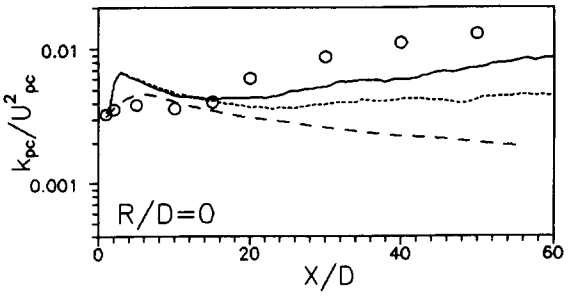

Figure 6. Particle turbulent kinetic energy (Shuen *et al.* 1983b). O, Experiment (Shuen *et al.*); ----, Anagnostopoulos & Bergeles (1988); ----, present method A; ——, present method B.

significant differences. This is logical since the flow field is rather simple. The results are from the 100 × 50 grid computations.

(ii) For Hardalupas *et al.* (1990), grid independence was achieved for a 35 × 40 grid, which is the same grid as used by Anagnostopoulos & Bergeles (1992). A finer grid was required compared to in the previous test because of the complexity of the flow (recirculation zone etc.).

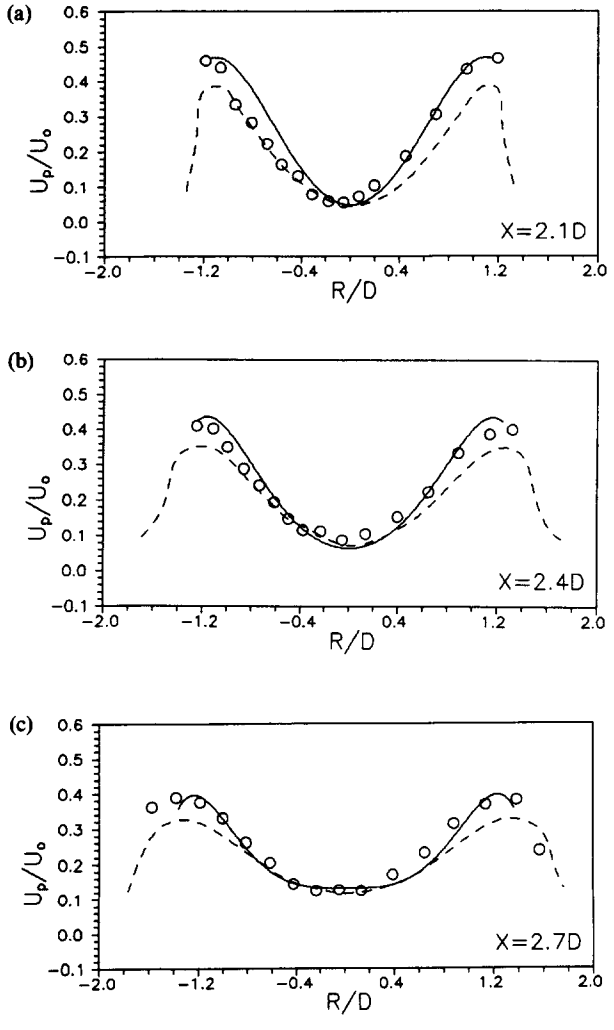

Figure 7(a–c). Particle axial velocities (Hardalupas *et al.* 1990). O, Experiment (Hardalupas *et al.*); ----, Anagnostopoulos & Bergeles (1992); ——, present method A and B.

The particles, however, were tracked in grids that were twice the size of the flow field's grid. This does not make convergence slower but gives better approximations for the results related to the particles. The time step used was also derived from this finer grid and taken to be small enough so that the particle would not leave a grid cell in only one step. Within this limitation the time step can be taken as large as possible due to the advantages of the model mentioned in previous sections.

A criterion of convergence of the flow field was that residual source terms of each velocity component and the residual mass source term became smaller than 0.3% of the inlet value. An example of the convergence is presented in figure 8 for the case of Hardalupas *et al.* (1990). The two-phase field was considered converged when two subsequent trackings (indicated by circles in figure 8) brought on no significant difference to the flow field and, thus, the field converged in very few iterations after the particles had been tracked. As previously mentioned, about 3–4 trackings were required.

It should be noted that although the 2000–5000 particle trajectories mentioned above are sufficient for the convergence of the flow field, about 10 times as many are then used to obtain statistically smooth curves depending on the type of field and on the mass loading.

Although the initial conditions for the particles were relatively well defined in the test cases that were considered, the "rough" assumption used to overcome the few undefined conditions (subsection 3.1) was the only possible solution and could be the cause of undesirable effects as mentioned above. Radial profiles of the initial conditions are not shown here due to lack of space, however they can be found in the corresponding references.

For the test case of subsection 3.1, the mass loading of 66% is quite large. However, we are dealing with particles that are relatively small and dense and, therefore, the particle–fluid volume fraction is small enough (0.03%) to permit the assumption that particle–particle interactions may be neglected. These interactions are probably negligable here, considering that particles of about the same density were well predicted by Sargianos *et al.* (1990) and by Berlemont *et al.* (1990) at a mass loading of 80 and 85% respectively, without taking particle interactions into account.

As expected, the CPU time for the present method was greater than for the previous methods, which assumed an isotropic character of the flow. On an IBM compatible 386-SX computer with a coprocessor of 20 MHz the previous method tracked 100 particles in about 3 min, while the present method needed about 3 times as much time. However, as discussed above, the tracking time step is directly related to the density of the grid and while the previous method demanded small time steps, the present one does not. This was not taken advantage of in the timing, since a larger time step would have caused the particle to exceed the limit of one grid cell in one step. A coarser grid for the particles could have been acceptable for the present method, leading to larger time steps and shorter CPU times.

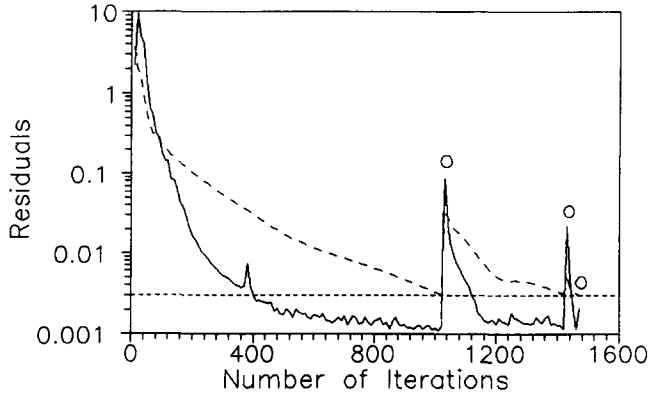

Figure 8. Flow field convergence of Hardalupas *et al.* (1990). ——, Mass residual; ----, *U* velocity residual; O, solid phase calculation.

5. CONCLUSIONS

A Lagrangian approach to the prediction of particle behaviour in anisotropic turbulence was presented. The new approach is three-dimensional and considers the effect of the anisotropy of the turbulence on the particles.

Following a particle trajectory requires knowledge related to the carrier phases fluctuating turbulent velocity. Temporal correlation of these fluctuations in subsequent time steps was introduced. Then the three components of the fluctuations were directionally correlated to account for the anisotropic influence. Heavier particles do not follow a fluid particle's trajectory and therefore fluid fluctuating velocities at their position must be derived from those at the fluid particle's position through a spatial correlation feature which is also incorporated.

The tests performed in sections 2.1 and 2.2 are definite proof as to the correct performance of the method when predicting anisotropic turbulence. In section 2.3 spatial correlation is introduced and the full model is used in section 3 to predict first a simple two-phase turbulent round free jet (Shuen *et al.* 1983b) and then a more complicated swirling flow from an unconfined quarl burner (Hardalpas *et al.* 1990). In that section, uncertainties arise with respect to the constants appearing in the correlation function. The results though imply that the use of anisotropic time and length scales does not make a significant difference and isotropic scales are quite adequate. However, a further investigation into this conclusion is considered important. Other areas that would probably influence the model are the Reynolds stress model and possible improvements in the correlation functions (the spatial correlation in particular).

The overall predictions were favourable and suggest that the model will prove useful in the prediction of anisotropic two-phase flows. Applications of this type of modelling (in the isotropic phase so far) are presently being performed at the National Technical University of Athens, simulating pulverized coal combustion in a furnace.

REFERENCES

ANAGNOSTOPOULOS, J. S. & BERGELES, G. C. 1988 Numerical study of particle-laden jets: a Lagrangian approach. In *Mathematical Modelling in Combustion and Related Topics* (Edited by C. M. Brauner and C. Shmidt-Laine). *NATO ASI Series E.* Martinus Nijhoff, The Hague.

ANAGNOSTOPOULOS, J. S. & BERGELES, G. C. 1992 Discrete-phase effects on the flow field of a droplet-laden swirling jet with recirculation: a numerical study. *Int. J. Heat Fluid Flow* **13,** 141–150.

BERLEMONT, A., DESJONQUERES, P. & GOUESBET, G. 1990 Particle Lagrangian simulation in turbulent flows. *Int. J. Multiphase Flow* **16,** 19–34.

DIAKOUMAKOS, H., ANAGNOSTOPOULOS, J. & BERGELES, G. 1988 A theoretical study of solid–air two-phase flow. In *Mathematical Modelling in Combustion and Related Topics* (Edited by C. M. Brauner and C. Schmidt-Laine). *NATO ASI Series E.* Martinus Nijhoff, The Hague.

GOSMAN, A. D. & IOANNIDES, E. 1981 Aspects of computer simulation of liquid-fuelled combustors. Presented at the *19th Aerospace Science Mtg*, St Louis, MO, AIAA Paper 81-0323.

HARDALUPAS, Y., TAYLOR, A. M. K. P. & WHITELAW, J. H. 1990 Velocity and size characteristics of liquid-fuelled flames stabilized by a swirl burner. *Proc. R. Soc. Lond.* **A428,** 129–155.

HINZE, J. O. 1975 *Turbulence*, 2nd edn. McGraw-Hill, New York.

KALIO, G. A. & STOCK, D. E. 1986 Turbulent particle dispersion: a comparison between Lagrangian and Eulerian modelling approaches. In *Proc. Gas–Solid Flow, the AIAA/ASME 4th Fluid Mechanics, Plasma Dynamics and Lasers Conf.*, Atlanta, GA, pp. 23–34.

LAUNDER, B. E. & SPALDING, D. B. 1974 The numerical computation of turbulent flows. *Comput. Meth. Appl. Mech. Engng* **3,** 269.

MEI, R., ADRIAN, R. J. & HANRATTY, T. J. 1991 Particle dispersion in isotropic turbulence under stokes drag and Basset force with gravitational settling. *J. Fluid Mech.* **225,** 481–495.

MILOJEVIC, D. 1990 Lagrangian stochastic-deterministic (LSD) Predictions of particle dispersion in turbulence. *Particles Particle Syst. Charact.* **7,** 181–190.

PICART, A., BERLEMONT, A. & GOUESBET, G. 1986 Modelling and prediction turbulence fields and the dispersion of discrete particles transported by turbulent flows. *Int. J. Multiphase Flow* **12,** 237–261.

SARGIANOS, N. P., ANAGNOSTOPOULOS, J. & BERGELES, G. 1990 Turbulence modulation of particles downstream of a two-phase, particle-laden, round jet. In *Proceedings of an International Symposium on Engineering Turbulence Modelling and Measurement, Dubrovnik* (Edited by RODI, W. & GANIC, E. N.), pp. 897–906. Elsevier, New York.

SHUEN, J. S., CHEN, L. D. & FAETH, G. M. 1983a Evaluation of a stochastic model of particle dispersion in a turbulent around jet. *AIChE Jl* **29,** 167–170.

SHUEN, J. S., SOLOMON, A. S. P., ZHANG, Q. F. & FAETH, G. M. 1983b A theoretical and experimental study of turbulent particle-laden jets. Report NASA CR-168293.

SMOOT, L. D. & PRATT, D. T. 1979 *Pulverized-coal Combustion and Gasification.* Plenum Press, New York.

YUU, S., YASUKOUCHI, N., HIROSAWA, Y. & JOTAKI, 1978 Particle turbulent diffusion in a dust laden round jet. *AIChE Jl* **24,** 509–519.

ZHOU, Q. & LESCHZINER, M. A. 1991 A time-correlated stochastic model for particle dispersion in anisotropic turbulence. In *Proc. 8th Symp. on Turbulent Shear Flows,* Munich, pp. 10-3-1–10-3-6.